Optical and ultrasonic monitoring of femtosecond laser filamentation in fused silica

Vygantas Mizeikis [a,*], Saulius Juodkazis [a], Tadas Balčiūnas [b], Sergey I. Kudryashov [c], Vladimir D. Zvorykin [c], Andrei A. Ionin [c], Hiroaki Misawa [a]

[a] *Research Institute for Electronic Science, Hokkaido University, N21W10 CRIS Bldg., Sapporo 001-0021, Japan*
[b] *Laser Research Center, Department of Quantum Electronics, Vilnius University, Sauletekio 9, LT-2040 Vilnius, Lithuania*
[c] *P.N. Lebedev Physical Institute, Russian Academy of Sciences, 119991 Moscow, Russia*

Abstract

Millimeter-long filaments and accompanying luminous plasma and defect channels created in fused silica (FS) by single focused femtosecond laser pulses with supercritical powers were probed in situ using optical imaging and contact ultrasonic techniques. Above the threshold pulse energy $E_{opt} = 5\,\mu$J corresponding to a few megawatt power levels pulses collapse due to self-focusing, producing channels filled by electron-hole plasma and luminescent defects, and exhibits predominantly compressive pressure transients. Analysis of the optical and ultrasonic response versus the laser pulse energy suggests that filamentary pulse propagation in the channels occurs with considerable dissipation of about $\sim 10\,\mathrm{cm}^{-1}$. The predominant ionization mechanism is most likely associated with avalanche ionization, while the main mechanism of optical absorption is free-carrier absorption via inverse Bremsstrahlung interaction with the polar lattice.

Key words: femtosecond filaments, silica glass, acoustic monitoring
PACS: 52.50.Jm, 61.82.Ms, 52.35.Dm, 52.38.Mf

Filamentation of femtosecond laser pulses in dielectric silica glass involves formation of micrometer-sized light bullets propagating over distances much longer than their diffraction length without any external guiding. Simultaneously, generation of extended electron-hole plasma (EHP) occurs in the narrow channels of micrometric cross sections. These channels are optically recognizable from their transient luminescence and from permanent modification in the materials' optical transparency via point defect generation or optical ablation [1,2]. Small spatio-temporal envelope of the filaments makes their detailed monitoring of EHP dynamics, one of the key characteristics of filaments in photoexcited dielectrics [1–3], difficult. It is helpful to note here, that dense plasmas are known to generate intense ultrasonic waves [4–6], which can reveal important parameters of the plasma. Ultrasonic probing has been applied fruitfully for remote monitoring of femtosecond laser filaments in air [7] and water [8], but comprehensive ultrasonic studies of filamentation in bulk dielectrics, to the best of our knowledge, have not yet been performed. We have conducted *in situ* optical and ultrasonic imaging of self-focusing and filamentation of single femtosecond laser pulses with supercritical pulse powers in fused silica. The samples used were blocks of fused silica (FS) glass (Seiken, Inc.) with refractive index $n_0 \approx 1.5$ at the wavelengths of 800 and 1030 nm [9]. The laser source was a Hurricane Ti:Sapphire am-

* Corresponding author
Email address: vm@es.hokudai.ac.jp (Vygantas Mizeikis).

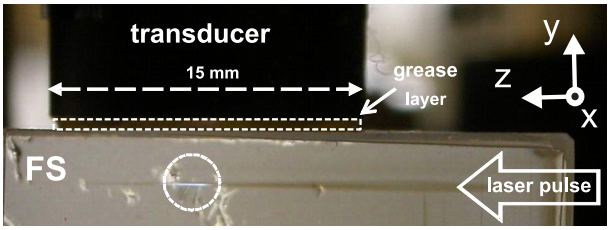

Fig. 1. Side-view optical image of the plasma channel (emphasized by the dashed circle), and optical damage traces (dark lines) in FS at the laser pulse energy $E = 20\,\mu$J. Ultrasonic imaging is done by an ultrasonic transducer, seen as the dark 15 mm-wide rectangle at the top surface of the FS sample.

plified laser system (Spectra Physics) producing pulses of $\tau_p \approx 150$ fs duration (FWHM) at an adjustable rate of up to $f = 1$ kHz and a central wavelength $\lambda_c = 800$ nm. Laser beam having the diameter of 7 mm was focused into the samples by a lens with a focal distance $F = 100$ mm, which allows one estimate lateral radius of the Gaussian beam waist at $1/e^2$ intensity level as $w_0 \approx 12\,\mu$m, and Rayleigh length $l_0 \approx 0.5$ mm.

The combined optical and ultrasonic monitoring experiments are further illustrated in Fig. 1. The laser beam entered the sample through the polished (right) side face along the $z-$axis direction. The sample was mounted on a translation stage, which was translated along the $x-$axis normal to the Figure plane, such that each incident pulse exposed fresh (previously not irradiated) regions of the sample. Optical monitoring was conducted along the $x-$axis through the front face of the sample by recording the images of the EHP plasma channels using an optical microscope and a digital photo camera. From the images, length, width, and intensity distribution within the plasma channels were determined. Ultrasonic response was recorded along the $y-$axis direction by MiniWAT-2 transducer (UC VINFIN) with sensitive area of (8×8) mm^2, sensitivity of about 10 V/atm, and effective bandwidth of $\Delta f \approx 30$ MHz, mounted on the flat top face of the glass sample, on which 0.3 mm thick layer of vacuum grease was deposited in order to ensure acoustic contact and mechanical lubrication. The beam waist formed a few millimeters below the center of the transducer. Relative positions of the laser beam and transducer were maintained the same during the experiments, independent of the lateral translation of the sample. Voltage transients from the transducer were recorded using Tektronix TDS-5104 digital storage oscilloscope, triggered by

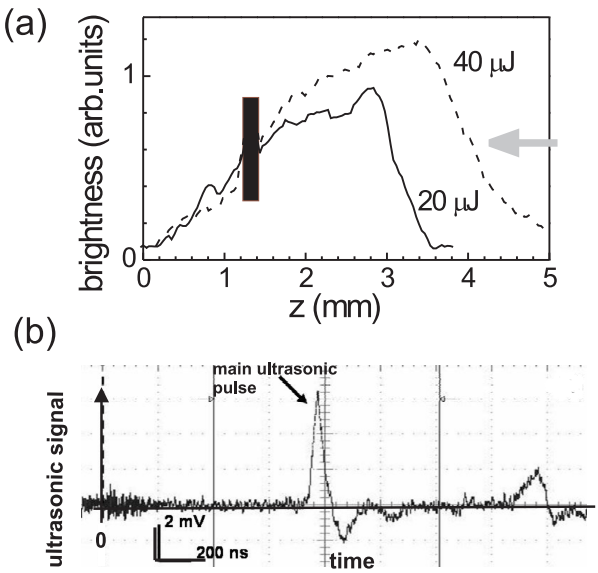

Fig. 2. Typical optical and ultrasonic signatures of luminous channels. (a) Radially-integrated channel brightness versus the axial (z) coordinate for two different pulse energies ($E = 20$ and $45\,\mu$J). The black box masks an artifact due to a scratch on the sample, the gray arrow indicates the pulse propagation direction. (b) Ultrasonic transient signal from a single laser pulses with energy of $E = 65\,\mu$J.

an auxiliary laser pulse via a fast photodiode.

Optical emission of the channels seen in Fig. 1 is known to originate from EHP and defects, exhibiting photoluminescence (PL) bands centered at 280, 400, 470, 550 and 630 nm wavelengths [10–13]. The channels emerge at pulse energies above the optical threshold value $E_{opt} = 5\,\mu$J ($P_{opt} = 30$ MW) at a distance of ≈ 60 mm from the $F = 100$ mm lens due to self-focusing, since critical self-focusing power in FS at 800 nm is $P_{crit} \approx 2$ MW [14]. However, the peak pulse intensity corresponding to E_{opt}, $I_{opt} \approx 5$ TW/cm^2, is still somewhat lower than the bulk FS optical breakdown/damage threshold of ≈50-60 TW/cm^2 [3,15].

Figure 2(a) shows axial (along the $z-$ axis) profiles of the channel brightness at pulse energies of $E = 20$ and $40\,\mu$J. The channels have a sharp leading edge, a plateau region, and a steep trailing edge. With increasing pulse energy the leading edge moves closer to the laser source (in Figs. 1 and 2 the beam enters the sample from right to left) due to self-focusing. The plateau extends from approximately 3.5 down to 1.5 mm, and has a length $b \approx 1 - 2$ mm. In optical observations this region constitutes the major part of apparent length of the channel. One can estimate $b \approx 1.2$ mm at $E = 20\,\mu$J, i.e.,

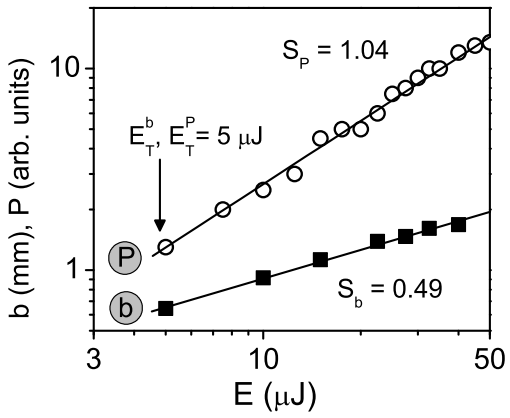

Fig. 3. Pulse energy dependencies of the ultrasonic compressive pressure P and the channel length b.

the channel length clearly exceeds linear Rayleigh length $l_0 \approx 0.5$ mm. The steep trailing edge at $y <$ 1.5 mm is nearly-exponential due to the laser beam dissipation characterized by an effective length of ~ 10 cm^{-1}. Diameter of the filaments determined from high-resolution micrographs of the channels (not shown) was found to be $a_{fil} \sim 10\,\mu$m, in agreement with the literature [1]. Hence, intensity at the non-linear focus of the beam $I_{opt}^{NL} = E_{opt}/a_{fil}^2\tau_p \approx$ 30 TW/cm^2 is sufficient for photo-ionization and generation of sub-critical EHP in FS [3,15].

Typical shape of the transient ultrasonic signal is shown in Fig. 2(b). The initial delay time (of 0.75 μs) before the arrival of the first pulse represents propagation from the channel (ultrasonic source) to the sample surface and across the layer of vacuum grease. The first asymmetric bipolar pulse represents major compression (positive) and minor rarefaction (negative) phases in FS within $t \approx 0.75 - 1.0\,\mu$s. The second bipolar pulse seen for times larger than 1 μs represents acoustic reverberations in the detector system. This circumstance was verified in separate experiments in which instrumental response of the sensor was measured by subjecting its intentionally blackened sensitive area to a 10 ns wide laser pulse, which generated purely compressive pressure at the sensor. The resulting electric pulse had a major compressive part and a minor negative oscillating part with a maximum amplitude of about 10%. Detailed description of these experiments goes beyond the scope of paper.

The first compressive pulse exhibits broadening with the laser pulse energy in the range of $\tau_{broad} = 45 - 110$ ns, indicating progressive elongation and translation of the ultrasonic source with respect to the transducer. At the same time, amplitude ratio of the rarefaction and compression signals remains nearly constant, and the source pressure is predominantly compressive, indicating that their origin is most likely generation of electron-ion plasma [8] or point defects [16] (other mechanisms, such as electronic stress generated by femtosecond pulses via the acoustic deformation potential [17] or thermoelastic stress [18] would result in symmetrically bipolar ultrasonic transients [18]). Magnitude of the negative phase in the instrumental response of the sensor (see above) indicates that at least half of the negative oscillatory signal after the positive pulse can be attributed to the sensor itself. Thus, the remaining negative signal representing rarefaction is by at least an order of magnitude weaker than the positive compression signal, and can be regarded as insignificant.

Temporal width of the compressive pulses reflects the largest possible spread of the path lengths between various segments of the linear ultrasonic source, and the detector plane. In these circumstances one can determine the effective length $b(E)$ of the ultrasonic source (channel), and the ultrasonic pressure $P(E)$ using a simple geometric analysis based on Pythagorean theorem [19]. Figure 3 shows the obtained $b(E)$ and $P(E)$ dependencies. The $b(E)$ dependence is well approximated by a square root law (with slope $S_b = 0.49$) of the form $b(E) = b_0\sqrt{E - E_T^b}$, where constant $b_0 \approx 0.28\,\text{mm}/\sqrt{\mu\text{J}}$ reflects dissipative losses in the channels. This dependence agrees well with the behavior of with optically visible channel length. Most importantly, it has the same threshold energy of $E_T^b = 5 \pm 1\,\mu$J $\approx E_{opt}$. The qualitative $P(E)$ dependence derived using the above arguments is shown in Fig. 3, and is linear above a threshold pulse energy $E_T^P = 5 \pm 1\,\mu$J the same as E_{opt} and E_T^b, thus confirming close physical relationship between the luminous channels and ultrasonic sources. Assuming energy-independent diameter of the ultrasonic channels, the ultrasonic source pressure scaling $\propto E^{0.79}$ can be obtained according to [20]. Similar scaling laws were found previously in sub-critical electron-ion plasmas [21]. In our case such scaling may indicate that laser energy deposition due to the warm sub-critical EHP absorption via inverse Bremsstrahlung effect predominates multi-photon

absorption (MPA).

These findings lead to the conclusion that filaments generated by loosely-focused fs laser pulses with supercritical powers in FS are filled EHP and/or luminescent point defects, and that EHP within the channels remains sub-critical (density of $N_e \sim 10^{20}\,\mathrm{cm}^{-3}$ was estimated for our experimental conditions, whereas the critical plasma density at the 800 nm wavelength is known to be $N_{crit} \approx 1.8 \times 10^{21}\mathrm{cm}^{-3}$ [1]). Scaling of the channel brightness with laser pulse energy $\propto E^{1/4}$ was observed, indicating strong role of the electron density in the generated EHP, in accordance to the literature [21]. In general, our observations are consistent with results of earlier studies of filamentation FS and other dielectrics under similar experimental conditions [1,4,5].

This work was supported by the following grants from the Ministry of Education, Science, Sports, and Culture of Japan: grant-in-aid No. 19360322 (to S. Juodkazis), and KAKENHI grant-in-aid for Scientific Research on Priority Area "Strong Photons-Molecules Coupling Fields" No. 470.

References

[1] A. Couairon, A. Mysyrowicz, Femtosecond filamentation in transparent media, Phys. Rep. 441 (2007) 47.

[2] L. Berge, S. Skupin, R. Nuter, J. Kasparian, J.-P. Wolf, Ultrashort filaments of light in weakly ionized, optically transparent media, Rep. Prog. Phys. 70 (2007) 1633.

[3] S. Mao, F. Quere, S. Guizard, X. Mao, R. Russo, G. Petite, P. Martin, Dynamics of femtosecond laser interactions with dielectrics, Appl. Phys. A 79 (2004) 1695.

[4] A. Babin, A. Kiselev, D. Kulagin, K. Pravdenko, A.N.Stepanov, Shock-wave generation upon axicon focusing of femtosecond laser radiation in transparent dielectrics, JETP Lett. 80 (2004) 298–302.

[5] A. Horn, E. Kreutz, R. Poprawe, Ultrafast time-resolved photography of femtosecond laser induced modifications in BK7 glass and fused silica, Appl. Phys. A 79 (2004) 923–925.

[6] M. Sakakura, M. Terazima, Y. Shimotsuma, K. Miura, K. Hirao, Observation of pressure wave generated by focusing a femtosecond laser pulse inside a glass, Opt. Exp. 15 (2007) 5674–5686.

[7] P. Yu, M. Cardona, Fundamentals of Semiconductors: Physics and Materials Properties, Springer, Berlin, 2002.

[8] E. Glezer, C. Schaffer, N. Nishimura, E. Mazur, Minimally disruptive laser-induced breakdown in water, Opt. Lett. 22 (1997) 1817–1819.

[9] E. D. Palik (Ed.), Handbook of Optical Constants of Solids, Academic Press, Orlando, 1998.

[10] N. Fukata, Y. Yamamoto, K. Murakami, M. Hase, M. Kitajima, In situ spectroscopic measurement of structural change in SiO_2 during femtosecond laser irradiation, Appl. Phys. A 79 (2004) 1425–1427.

[11] A. Zoubir, C. Rivero, R. Grodsky, K. Richardson, M. Richardson, T. Cardinal, M. Couzi, Laser-induced defects in fused silica by femtosecond IR irradiation, Phys. Rev. B 73 (2006) 224117.

[12] M. Watanabe, S. Juodkazis, H.-B. Sun, S. Matsuo, H. Misawa, Luminescence and defect formation by visible and near-infrared irradiation of vitreous silica, Phys. Rev. B 60 (14) (1999) 9959–9964.

[13] W. Reichman, D. Krol, L. Shah, F. Yoshino, A. Arai, S. Eaton, P. Herman, A spectroscopic comparison of femtosecond-laser-modified fused silica using kilohertz and megahertz laser systems, J. Appl. Phys. 99 (2006) 123112.

[14] A. Couairon, L. Sudrie, M. Franco, B. Prade, A. Mysyrowicz, Filamentation and damage in fused silica induced by tightly focused femtosecond laser pulses, Phys. Rev. B 71 (2005) 125435.

[15] M. Li, S. Menon, J. Nibarger, G. Gibson, Ultrafast electron dynamics in femtosecond optical breakdown of dielectrics, Phys. Rev. Lett. 82 (1999) 2394–2397.

[16] W. Hayes, A. Stoneham, Defects and Defect Processes in Nonmetallic Solids, Dover, New York, 2004.

[17] C. Thomsen, H. Grahn, H. Maris, J. Tauc, Surface generation and detection of phonons by picosecond light pulses, Phys. Rev. B 34 (1986) 4129–4138.

[18] A. Vogel, J. Noack, G. Hütman, G. Paltauf, Mechanisms of femtosecond laser nanosurgery of cells and tissues, Appl. Phys. B 81 (2005) 1015–1047.

[19] V. Mizeikis, S. Juodkazis, T. Balčiunas, H. Misawa, S. Kudryashov, V.D.Zvorykin, A. Ionin, *to be published* (2008).

[20] V. Gusev, A. Karabutov, Laser Optoacoustics, AIP, New York, 1993.

[21] C. Phipps, T. Turner, R. Harrison, G. York, W. Osborne, G. Anderson, X. Corlis, L. Haynes, H. Steele, K. Spicochi, Impulse coupling to targets in vacuum by KrF, HF, and CO_2 single-pulse lasers, J. Appl. Phys. 64 (1988) 1083.